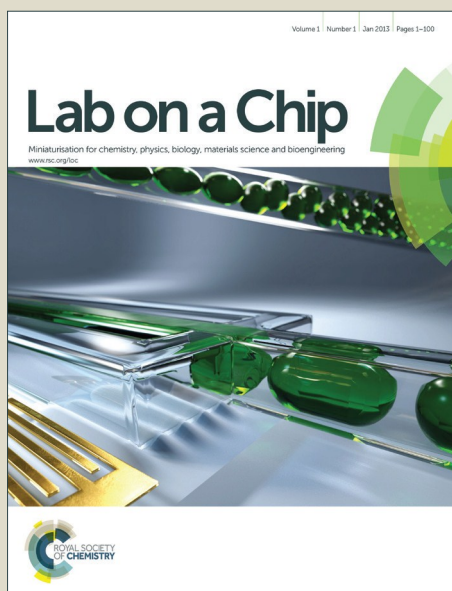


Lab on a Chip

Accepted Manuscript



This is an *Accepted Manuscript*, which has been through the Royal Society of Chemistry peer review process and has been accepted for publication.

Accepted Manuscripts are published online shortly after acceptance, before technical editing, formatting and proof reading. Using this free service, authors can make their results available to the community, in citable form, before we publish the edited article. We will replace this *Accepted Manuscript* with the edited and formatted *Advance Article* as soon as it is available.

You can find more information about *Accepted Manuscripts* in the [Information for Authors](#).

Please note that technical editing may introduce minor changes to the text and/or graphics, which may alter content. The journal's standard [Terms & Conditions](#) and the [Ethical guidelines](#) still apply. In no event shall the Royal Society of Chemistry be held responsible for any errors or omissions in this *Accepted Manuscript* or any consequences arising from the use of any information it contains.

Tumor Cell Targeting Peptide Ligands Distinguishing through Color-Encoding Microarray[†]

S1Received 00th January 20xx,
Accepted 00th January 20xx

DOI: 10.1039/x0xx00000x

Zihua Wang^{§a}, Weizhi Wang^{§*a}, Lingling Geng^a and Zhiyuan Hu^{**a}

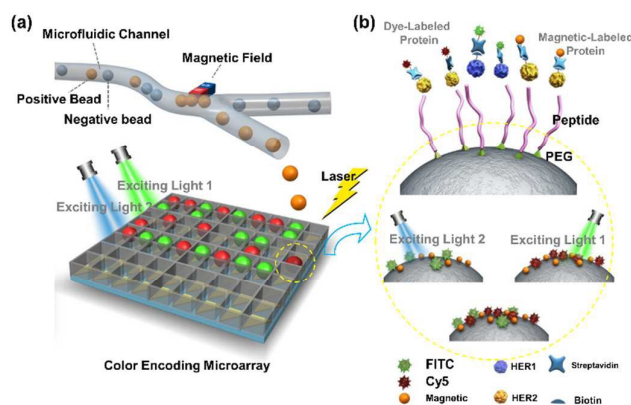
www.rsc.org/

One silicon-based microarray system was constructed to discover the affinity peptides and to distinguish the specific peptides from the high throughput library. Using the color-encoding strategy, *in situ* peptide distinguishing between the HER1 ligands and HER2 ligands was achieved. Novel affinity peptide sequences H1P (HER1 ligand) and H2P (HER2 ligand) were determined with nmol affinity.

Small molecular ligands are important tools for studying complex biological functions.^{1, 2} As excellent small molecular ligands, peptides are low-immunogenic and low-toxicity reagents in living system. Conventionally, affinity peptide ligands could be screened out through combinatorial library of which the “one bead one compound” (OBOC) strategy is the most common one.³ However, the on-bead screening against macromolecular targets is highly susceptible to interference from nonspecific interactions between the target molecule and the bead surface (which are defined as aimless interactions other than the intended interaction), resulting in biased screening data or in some cases, complete failure of the screening experiment.⁴⁻⁶ As a result, an accurate peptide screening process without false positive hits is highly desirable. Recently, several approaches have been developed for the fragment-based discovery to perform accurate ligands screening.^{7,8} With the development of micro electromechanical systems (MEMS) and large scale integration (LSI), precise ligand screening could be performed integrately. Therein, small-molecule microarrays provide an efficient strategy for high-throughput and high-content molecular interactions.^{9, 10} Since the microarray-based detection can considerably increase throughput and allow for simultaneous data acquisition, the strategy could be employed to screen and identify the “true” specific peptide ligands towards biomarkers from a large number of molecules.^{11,12}

Herein, the biomarker epidermal growth factor receptor (EGFR) is what we are interested in. EGFR family consists of four homologous members: HER1,HER2, HER and HER4.¹³ These receptors are essential in modulating cell proliferation and cell differentiation in

tissues.^{14,15} Among them, aberrant expression of HER1 and HER2 has been implicated in the development of many types of human cancers, including breast, lung, pancreatic, and ovarian cancers.^{16,17} Therefore, HER1 and HER2 have been intensely pursued as therapeutic targets. However, the sequence homology between HER1 and HER2 in the extracellular domain is 44% and as high as 82% in the kinase domain.¹⁸ Therefore, it is difficult to screen the specific ligands towards the HER1 or HER2, respectively. Some affinity peptide towards HER1 is also the ligands of HER2.¹⁹



Scheme 1 The principle of the microarray screening process. (a) Each well in the microarray was designed half transparent and half conductive (b) Each of the positive bead was labelled by different colors indicating the specificity

As shown in Scheme 1a, we report here a silicon-based microarray to discover the affinity peptides and to distinguish the specific peptides from 10⁵ OBOC combinatorial library using the color-encoding strategy in a direct-reading way. Novel affinity peptides H1P (HER1 ligands) and H2P (HER2 ligand) were determined specifically.

In the first stage, a 10-mer OBOC peptide library was constructed through the solid phase peptide synthesis (SPPS) strategy.^{4, 20} The library was served as X₁ X₂ X₃ X₄ X₅ X₆ X₇ X₈ CGM in which the sequences on each bead would be randomly distributed result from the “split and pool” approach. The details of the sequences and the synthesis process was described in Scheme S1. High-throughput screening was performed from approximately 4.8 × 10⁵ candidate peptide beads. In order to realize an unbiased display of free molecular geometries, the interactions between the affinity

^a CAS Key Laboratory for Biomedical Effects of Nanomaterials & Nanosafety, National Center for Nanoscience and Technology of China Beijing 100190, China.
[§] The two authors contributed equally.

* Corresponding author. Fax: +86-10-82545643; Tel: +86-10-82545643; E-mail: huzy@nanocn.cn, wangwz@nanocn.cn.

[†] Electronic Supplementary Information (ESI) available: [some experimental details and some additional results]. See DOI: 10.1039/x0xx00000x

peptides and protein were mediated by biotin-streptavidin conjugation followed the previous procedure.²¹⁻²³ As shown in Scheme 1b, biotinylated HER2 was incubated with the streptavidin-magnetic beads to prepare a “magnetic-HER2”. In addition, biotinylated HER2 was incubated with the streptavidin-coated Cy5 (Cy5-HER2) while biotinylated HER1 was incubated with the streptavidin-coated FITC (FITC-HER1). A small amount of magnetic-HER2 were introduced into the library to process the preliminary screening. The HER2 coated magnetic beads will give the positive beads magnetic surfaces through which they could be isolated out of the library using magnetic separation approaches in a continuous-flow microfluidic process (Scheme 1a). All the beads in the library were introduced into the sorting micro channel (Scheme 1a, upper part). Positive peptide beads were enriched and isolated by a magnetic field. So that positive beads were trapped and adhere to one side of the tube while negative beads were flushed out. The positive beads were then collected and the streptavidin coated magnetic beads were removed from the beads system by centrifuge process.³ In this way, about 800 positive beads were isolated from the library. Meanwhile, equimolar Cy5-HER2 and FITC-HER1 were introduced to recognizing the true positive peptide beads.

The *in situ* detection was performed in a microarray. As shown in Scheme 1a as well as Figure 1a and b, a silicon-based microchip with high-density microarrays was designed and fabricated. The lab-on-chip system is consisted of *in situ* trapping, fluorescent analyses and peptide sequencing by MALDI-TOF-MS (matrix assisted laser desorption ionization time of flight mass spectrometry) detection. The microarray was divided into eight regularly arranged sub-arrays with 10×10 wells of each. Each well was designed with a cube shape with the dimension of 230 μm (L) × 230 μm (W) × 200 μm (D) which is exactly fit the single peptide bead in order to trap the beads in one-well-one-bead manner. The microwells were fabricated by conventional lithography procedure (Scheme S2). In order to realize the *in situ* single bead detection through optical means. Half of each microwell was etched through along the diagonal of the cube bottom. To ensure a good conductivity for MALDI-TOF detection, a silver layer of 200 nm thickness was sputtering on the surface of the microarray including the inner surface of the microwells. Along the diagonal, transparent half of the microwell was employed for *in situ* fluorescent detection and the other half was utilized for single bead MALDI-TOF-MS sequencing. Therefore, the microarray chip worked in a bi-functional manner.

The 800 positive beads from the library were loaded into the microarray by scraping the beads suspension back and forth until all the beads were trapped in the microwells. As shown in Figure 1, the fluorescent detection was carried out first and the fluorescent of each well was read through both Cy5 channel (red) and FITC channel (green). Although the peptide beads were trapped by the magnetic-HER2, different colors and different intensities were still revealed. It is indicated that a number of the false positive beads were sneaked during the preliminary screening. However, the fluorescent signal of the “true” positive beads will be “switched on” in a specific way because HER1 and HER2 was encoded by different colors. Also, the affinity of the peptide towards HER1 and HER2 could be indicated by the fluorescent intensity in a quantitative manner. In the color encoding microarray, about 40% of the beads revealed affinities towards HER2 (red fluorescent spots) and 30% of

the beads revealed affinities towards HER1 (green fluorescent spots). Among them, 10% of the ones show the both affinity towards the two proteins.

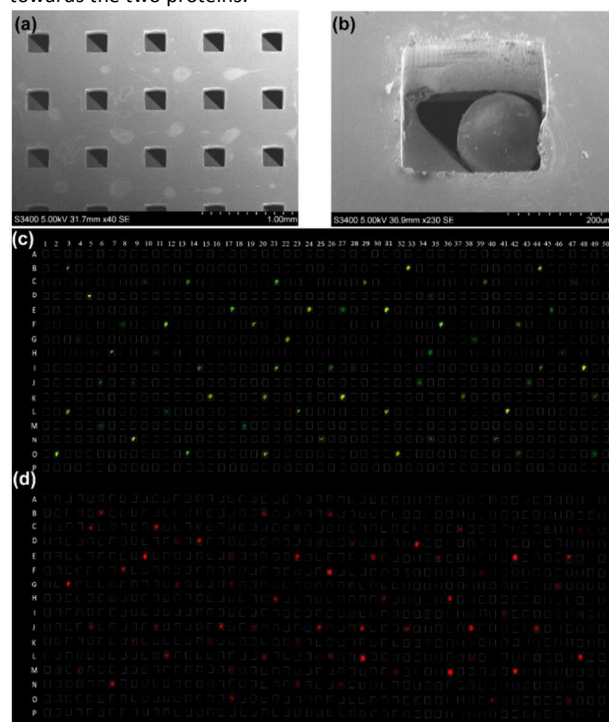


Figure 1 (a) SEM image of the fabricated structure of the microarray chip (b) SEM image of the “one-well-one bead” trapping (c) The red fluorescent detection of the color encoding microarray (Cy5 Channel) (d) The green fluorescent detection of the color encoding microarray (FITC Channel)

Guided by the fluorescent detection results, peptides were sequenced by MALDI-TOF-MS and the mass spectra of specific well could be obtained automatically. For Cy5 channel, about 150 TOF-TOF MS spectra were obtained through the detection of red fluorescent spots with relatively higher intensities. For FITC channel, about 130 TOF-TOF MS spectra were obtained. 50 spectra with both the signals were also confirmed. Figure S1 show the representative MS/MS spectra of the three model peptides.

For each condition, top 17 sequences, which hit the most probabilities, were aligned in the sequence map using the software *ClustalX 2* (Figure 2). As a result, peptide AHDFEHLHCG (named here H1P) were determined as the specific HER1 ligand and peptide NWRKTWLHCG (named here H2P) were chosen as the specific HER2 ligand. Peptide YWRFEWNRCG (named here HMP) were considered as the non-specific peptide because it showed affinities towards the two proteins. The affinities of the peptides towards protein HER1 and HER2 were determined by SPRI (Surface Plasmon Resonance imaging) detection. The dissociation constants (K_D s) were calculated.²² As shown in Figure 2, a, b and c represent the three peptides, H1P, H2P and HMP, respectively. For each peptide in the figure, the SPR curves towards HER1 were shown at upper right and SPR curves towards HER2 were shown at low right. K_D of H1P towards HER1 was calculated as 8 nM (nmol/L) and K_D of H2P towards HER2 was calculated as 116 nM. For the non-specific peptide HMP, the K_D towards HER1 was 4.6 nM and the K_D towards

HER2 was 810 nM. Either of the peptides H1P or H2P showed specific affinities towards HER1 or HER2 respectively. It is indicated that the peptide shown nano molar dissociation constants towards the target protein that are comparable to antibodies. The true

positive sequences could be pointed out in a precise and effective way by color encoding screening. The low dissociation constant has achieved a good binding affinity between the small ligands and large molecules.

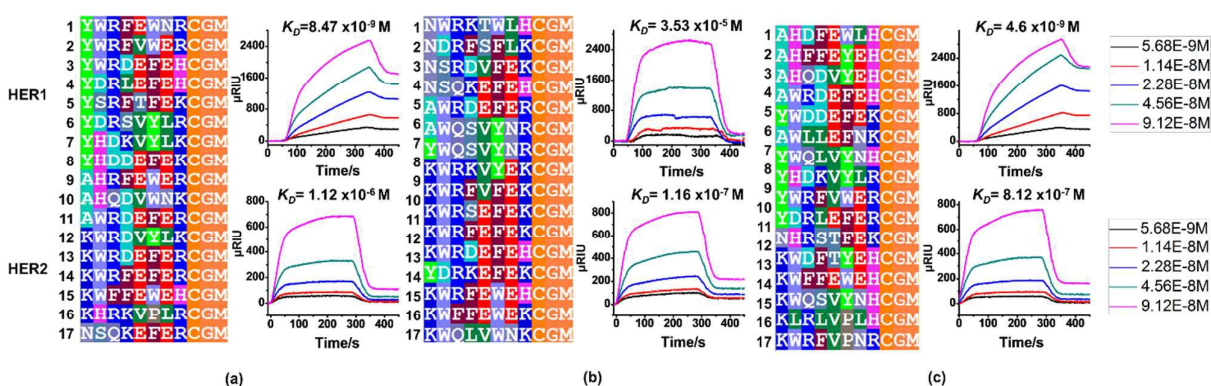


Figure 2. Alignment of sequences and the affinity determination of the peptides using SPRI. (a) The alignment of the sequences to HER1 (left), SPRI curves of H1P towards HER1 (upper right) and HER2 (low right); (b) The alignment of the sequences to HER2 (left), SPRI curves of H2P towards HER1 (upper right) and HER2 (low right); (c) The alignment of the sequences to both HER1&HER2 (left), SPRI curves of HMP towards HER1 (upper right) and HER2 (low right).

Further confirmation of the affinity peptides towards corresponding proteins were made in living cancer cells. Human breast cancer cell line MDA-MB-468 with high HER1 expression and human breast cancer cell line SKBR-3 with high HER2 expression were tested as models. Meanwhile, FITC labelled peptide (1 mg/mL), hoechest33342 (10 μ g/mL) and PE (Phycoerythrin) labelled antibodies (5 μ g/mL) were incubated with the above cells at 4 $^{\circ}$ C for 30 min and then rinsed with cold PBS three times. Confocal laser scan microscopy imaging was carried out in the excitation wavelength of 405 nm (Hoechst33342), 488 nm (FITC) and the 565 nm (PE). The fluorescent images were obtained at the emission wave length of 425 nm, 525 nm and 670 nm, respectively. For the MDA-MB-468 cell assay, H1P shows high green fluorescent signal towards HER1 positive cells while H2P shows little signal (Figure 3a and b). In addition, peptide and anti-HER1 antibody were co-localized on the membranes. The merged fluorescent signals further proved that the specific binding sites of the peptide ligands H1P is HER1 protein. For the SKBR-3 cell assay, it was exactly opposite. It is indicated that the specific binding sites of the peptide ligand H2P is HER2 protein (Figure 3d and e). Not surprisingly, the non-specify peptide HMP was binding on the cell membranes in both cell lines (Figure 3c and f). It is suggested that the high cellular uptake of the peptides were facilitated through HER1 or HER2 in a specific way. To check the specificity of the H1P, H2P and HMP, human embryonic kidney cell lines 293A (HEK) with no expression of HER1 and HER2 was served as negative cells. As illustrated in Figure S2 none of the peptides showed binding to the cell surface. It was revealed that the three peptides binding to HER1 and HER2 protein respectively with a specific manner. So H1P and H2P were very good molecular probes towards the cancer related biomarkers. The low toxicities of the peptide probes were also confirmed by MTT assay (Figure S3). To further explore the influence of the H2P peptide on cell growth process, growth curves were drawn. There is no obvious difference in cells treated with H2P compared with untreated ones (Figure S4).

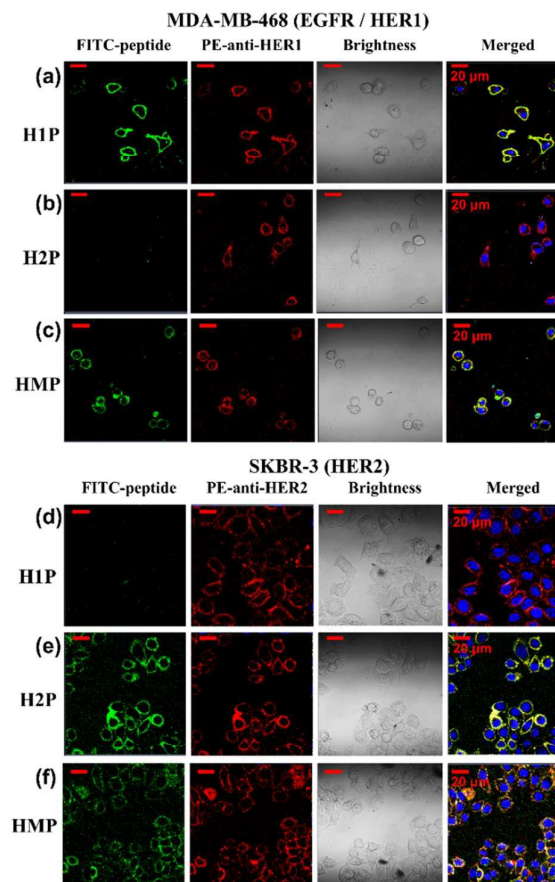


Figure 3. Confocal images of FITC-peptides and PE-antibodies towards living cancer cells. (a-c) FITC-H1P, FITC-H2P and FITC-HMP towards MDA-MB-468 cells with PE-anti-HER1 co-localized; (d-f) FITC-H1P, FITC-H2P and FITC-HMP towards SKBR-3 cells PE-anti-HER2 co-localized.

To further confirm the theoretical binding affinity and the binding site of the peptides towards the proteins, interaction energy was calculated from computer simulation using MM/GBSA method (Figure S5).²⁴ It showed that the predicted binding free energy of H1P/HER1 and H2P/HER2 is -40.12 ± 4.00 Kcal/mol and -43.56 ± 3.53 Kcal/mol, respectively. It is indicated that the ligand-receptor pairs H1P-HER1 and H2P-HER2 showed the stable bindings. As shown in Figure 4, decomposing of the binding site into individual residues was also done by the simulation of the crystal structures. The analysis indicated that the interaction of residues with His2-Met86, Glu5-Arg284, Trp6-His279 and Leu7-Val283 contribute most to the binding between H1P and HER1. The interaction of residues with Trp2-Gln84, Arg3-Leu291, Lys4-Gln59 and His8-Phe236 contribute most to the binding between H2P and HER2. The binding residues of H1P-HER1 and H2P-HER2 is quite different, which resulted in the specific bindings of the peptides towards specific proteins.

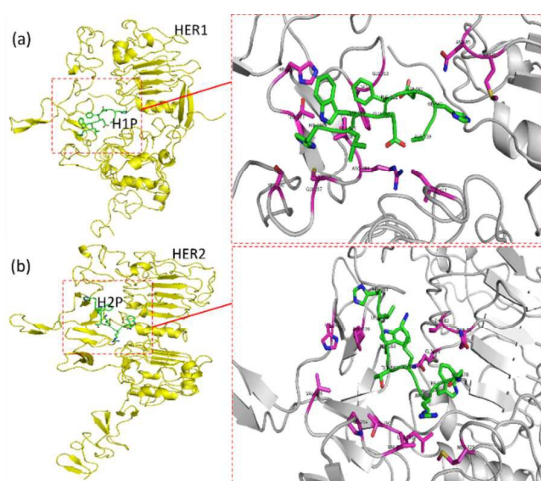


Figure 4. Three-dimensional representation of a peptide-protein. White cartoon and transparent surface: HER1/HER2, peptide is displayed as a green frame. (a) HER1/H1P complex. (b) HER2/H2P complex.

Conclusions

The color-encoding microarray system shows a prospective application for almost all types of peptide screening and determination. The novel peptide probes were prospectively employed for clinical use. In above, our work provides a new insight into the establishment of effective and universal strategy for screening small molecule probes.

Acknowledgement

We acknowledge funding from Beijing Municipal Natural Science Foundation (2144058), the National Natural Science Foundation of China (21305023, 31270875 and 31470049).

References

1. A. Herrmann, *Chem. Soc. Rev.*, 2014, **43**, 1899-1933.
2. S. Lee, X. Zheng, J. Krishnamoorthy, M. G. Savelieff, H. M. Park, J. R. Brender, J. H. Kim, J. S. Derrick, A. Kochi, H. J. Lee, C. Kim, A.

- Ramamoorthy, M. T. Bowers and M. H. Lim, *J. Am. Chem. Soc.*, 2014, **136**, 299-310.
3. J. M. Astle, L. S. Simpson, Y. Huang, M. M. Reddy, R. Wilson, S. Connell, J. Wilson and T. Kodadek, *Chem. Biol.*, 2010, **17**, 38-45.
4. X. Chen, P. H. Tan, Y. Zhang and D. Pei, *J. Comb. Chem.*, 2009, **11**, 604-611.
5. A. Furka, F. Sebestyén, M. Asgedom and G. Dibó, *Int. J. Pept. Protein Res.*, 1991, **37**, 487-493.
6. S. Nagrath, L. V. Sequist, S. Maheswaran, D. W. Bell, D. Irimia, L. Ulkus, M. R. Smith, E. L. Kwak, S. Digumarthy, A. Muzikansky, P. Ryan, U. J. Balis, R. G. Tompkins, D. A. Haber and M. Toner, *Nature*, 2007, **450**, 1235-U1210.
7. S. Ng, E. Lin, P. I. Kitov, K. F. Tjhung, O. O. Gerlits, L. Deng, B. Kasper, A. Sood, B. M. Paschal, P. Zhang, C.-C. Ling, J. S. Klassen, C. J. Noren, L. K. Mahal, R. J. Woods, L. Coates and R. Derda, *J. Am. Chem. Soc.*, 2015, **137**, 5248-5251.
8. C. Bodenreider, D. Beer, T. H. Keller, S. Sonntag, D. Wen, L. Yap, Y. H. Yau, S. G. Shochat, D. Huang, T. Zhou, A. Caflich, X.-C. Su, K. Ozawa, G. Otting, S. G. Vasudevan, J. Lescar and S. P. Lim, *Anal. Biochem.*, 2009, **395**, 195-204.
9. C. J. Zhang, C. Y. J. Tan, J. Y. Ge, Z. K. Na, G. Y. J. Chen, M. Uttamchandani, H. Y. Sun and S. Q. Yao, *Angew. Chem. Int. Edit.*, 2013, **52**, 14060-14064.
10. T. M. Doran and T. Kodadek, *ACS. Chem. Biol.*, 2014, **9**, 339-346.
11. M. B. Scheible, G. Pardatscher, A. Kuzyk and F. C. Simmel, *Nano. Lett.*, 2014, **14**, 1627-1633.
12. J. L. Garcia-Cordero and S. J. Maerkl, *Lab Chip*, 2014, **14**, 2642-2650.
13. T. Barrett, Y. Koyama, Y. Hama, G. Ravizzini, I. S. Shin, B.-S. Jang, C. H. Paik, Y. Urano, P. L. Choyke and H. Kobayashi, *Clin. Cancer Res.*, 2007, **13**, 6639-6648.
14. P. Casalini, M. V. Iorio, E. Galmozzi and S. Ménard, *J. Cell. Physiol.*, 2004, **200**, 343-350.
15. J. K. Scott and G. P. Smith, *Science*, 1990, **249**, 386-390.
16. A. S. D. S. Indrasekara, B. J. Paladini, D. J. Naczynski, V. Starovoytov, P. V. Moghe and L. Fabris, *Adv. Healthc. Mater.*, 2013, **2**, 1370-1376.
17. N. E. Hynes and H. A. Lane, *Nat. Rev. Cancer*, 2005, **5**, 341-354.
18. T. Yamamoto, S. Ikawa, T. Akiyama, K. Semba, N. Nomura, N. Miyajima, T. Saito and K. Toyoshima, *Nature*, 1986, **319**, 230-234.
19. D. Kim, Y. Yan, C. A. Valencia and R. Liu, *Plos One*, 2012, **7**.
20. R. W. Liu, J. Mark and K. S. Lam, *J. Am. Chem. Soc.*, 2002, **124**, 7678-7680.
21. W. Wang, Z. Wei, Z. Wang, H. Ma, X. Bu and Z. Hu, *RSC Adv.*, 2015, **5**, 5053-5053.
22. W. Wang, Z. Wei, D. Zhang, H. Ma, Z. Wang, X. Bu, M. Li, L. Geng, C. Lausted, L. Hood, Q. Fang, H. Wang and Z. Hu, *Anal. Chem.*, 2014, **86**, 11854-11859.
23. W. Wang, M. Li, Z. Wei, Z. Wang, X. Bu, W. Lai, S. Yang, H. Gong, H. Zheng, Y. Wang, Y. Liu, Q. Li, Q. Fang and Z. Hu, *Anal. Chem.*, 2014, **86**, 3703-3707.
24. D. Seeliger and B. de Groot, *J. Comput. Aided Mol. Des.*, 2010, **24**, 417-422.